PHYSICAL REVIEW B VOLUME 51, NUMBER 24 15 JUNE 1995-II

Electronic structure and optical properties of α and β phases of silicon nitride, silicon oxynitride, and with comparison to silicon dioxide

Yong-Nian Xu and W. Y. Ching

Department of Physics, University of Missouri–Kansas City, Kansas City, Missouri 64110

(Received 30 January 1995)

The electronic structure and the optical properties of α-Si_3N_4, β-Si_3N_4, and Si_2N_2O crystals are studied by means of first-principles local-density calculations. Together with the earlier published result on α-SiO_2, a comparative study of the electronic bonding and optical excitations in these crystals becomes possible. It is found that the electronic structure of the β and the α phases of Si_3N_4 are similar, but with some subtle differences that can be traced to different stacking sequences of the atomic layers and the slightly different local bonding structure. The electronic structure of the Si_2N_2O crystal cannot be adequately described as a simple superposition of Si_3N_4 and α-SiO_2. The presence of both Si—N and Si—O bonds in Si_2N_2O crystals affects the local potential and results in a downward shift of the O levels. The calculated density of states (DOS) and the orbital-resolved partial DOS are in good general agreement with the photoemission and x-ray emission measurements. Better resolution in the calculated DOS shows that the upper valence band has five peaks rather than three. Effective charge calculation suggests the ionic formulas of the four crystals to be α-$(Si^{+2.52})_3(N^{-1.89})_4$, β-$(Si^{+2.50})_3(N^{-1.87})_4$, α-$(Si^{+2.60})(O^{-1.30})_2$, and $(Si^{+2.54})_2(N^{-1.90})_2(O^{-1.25})$. The calculated optical properties of the four crystals show similar features in the gross absorption spectra but with differences in the peak positions. It is shown that all four crystals have intrinsic absorption tails, and those of Si_2N_2O and α-SiO_2 are larger than those of α-Si_3N_4 and β-Si_3N_4. This is explained by the nature of the wave function at the conduction-band minimum. The difference in the intrinsic band gap and the extrapolated optical gap is pointed out. Comparison with experimental data on amorphous Si_3N_4 shows good agreement with the optical conductivity of the crystalline phases. It is also shown that Si_2N_2O and α-SiO_2 crystals have negligible optical anisotropy, while for α-Si_3N_4 and β-Si_3N_4 the in-plane component of the dielectric function in the long-wavelength limit is smaller than the corresponding component parallel to the c axis. The calculated refractive indices are in good agreement with the limited data available.

I. INTRODUCTION

Silicon nitride (Si_3N_4) and silicon oxynitride (Si_2N_2O) are important structural ceramics with many modern applications. Si_3N_4 is used in automobile engines parts, cutting tools, machine components, nuclear reactors, etc., because of its superior mechanical, thermal, chemical, corrosion resistance and other outstanding high-temperature properties.[1-3] They also play an increasingly important role in the electronics industry, especially in Si-based large-scale integration circuit technology,[4] and possibly in optoelectronics.[5] Silicon oxynitride films have been considered for metal-nitride-oxide-silicon nonvolatile memory technology[6] and as optical wave guides.[7] Si_3N_4 is usually prepared from the high-temperature reaction-bond or hot-pressed sintering process and is therefore always in polycrystalline form with many defects and imperfections. Those prepared by chemical vapor deposition (CVD) are likely to be amorphous. The polycrystalline Si_3N_4 has two forms, α and β with β-Si_3N_4 to be thermodynamically more stable.[8] Both the α and β phases have the same basic structural units with a tetrahedral bonding for Si (Si—N_4) and a planer bonding for N (N—Si_3). The unit cell of the α phase is twice as large as the β phase, and they differ in the stacking sequence of the layer subunits along the c axis. For the β phase, the stacking is of the type $ABAB\ldots$, while for the α phase it is of the type $ABCDABCD$. The α-Si_3N_4 has a slightly buckled planer SiN_3 unit. The Si_2N_2O crystal can be considered as an intermediate phase between SiO_2 and Si_3N_4. The orthorhombic unit cell contains four formula units in a networklike structure such that the $[Si_2N_2]_n$ sheets in the y-z plane are linked together by bridging O along the x direction, while the Si atoms retain the tetrahedral bonding unit of O—Si—N_3. In Fig. 1, we depict the unit cells of the three crystals with different stacking layers.

The crystal parameters of both phases of Si_3N_4 (Refs. 9–14) and that of Si_2N_2O (Refs. 15 and 16) are well determined by several groups. Different reports differ only slightly in lattice constants and internal parameters which result in some differences in the computed bond lengths and bond angles. The structural information about these crystals used in the present calculation together with that of α-quartz (α-SiO_2) are summarized in Table I. The perfect crystalline Si_3N_4, SiO_2, and Si_2N_2O phases serve as pure reference systems for studying the properties of real silicon nitride ceramics which are inherently imperfect. Recent progress in material processing resulted in high quality films of amorphous Si_3N_4 (a-

0163-1829/95/51(24)/17379(11)/$06.00 ©1995 The American Physical Society

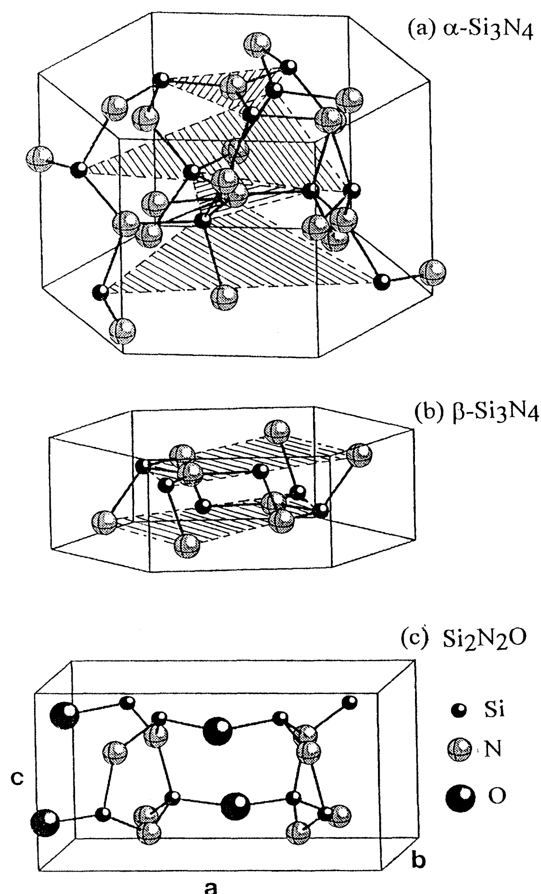

FIG. 1. Crystal structure of (a) α-Si_3N_4, (b) β-Si_3N_4, and (c) Si_2N_2O. Shaded planes indicate layer subunits perpendicular to the c axis.

Si_3N_4) which are used mainly as substrate materials.[17,18] Si_2N_2O may also appear as a secondary phase in the interfacial grain boundary of β-Si_3N_4. This has great implications on the overall performance of silicon nitride-based structural ceramics.[19] Recently, it has been recognized that SiO_xN_y glass can be an important optical material because of the possibility of varying the optical gap depending on the composition.[20] The properties of amorphous Si_3N_4 and SiO_xN_y with and without hydrogen doping have been extensively studied in recent years both theoretically[21–24] and experimentally.[25–44]

In contrast to α-SiO_2, the electronic structure of crystalline Si_3N_4 and Si_2N_2O phases has not been extensively studied. Back in 1982, Ren and Ching calculated the electronic structure of β-Si_3N_4 α-Si_3N_4 (Ref. 45), Si_2N_2O and Ge_2N_2O (Ref. 46) crystals using a first-principles method. Band structures and the density of states (DOS) for these crystals were presented. However, these calculations were not self-consistent, even though the crystal potentials were carefully constructed to give an accurate representation of the interaction. A self-consistent calculation for β-Si_3N_4 was carried out later which included the total-energy calculation[47] and valence charge distributions.[48] DOS calculations on crystalline and amorphous Si_3N_4 using empirical or semiempirical methods were carried out by several groups.[49,50,21–23] Robertson has thoroughly reviewed these calculations.[24] In addition, the effect of defects and doping elements in Si_3N_4 and related materials was also discussed. Tanaka *et al.* studied the electronic structure of β-Si_3N_4 using the discrete-variational $X\alpha$ method on small clusters.[51] Lately, Lui and Cohen performed a first-principles calculation of the electronic and structural properties of β-Si_3N_4 using the pseudopotential-localized orbital method.[52] The dynamic properties of β-Si_3N_4 and its implication on the pressure-

TABLE I. Comparison of crystal structure information of β-Si3N4, α-Si_3N_4, α-SiO_2, and Si_2N_2O crystals. The numbers in parentheses indicate the estimated ionic radius in Å in the Q^* calculation.

Crystal	α-Si_3N_4	β-Si_3N_4	α-SiO_2	Si_2N_2O
Lattice constant (Å)				
a:	7.766	7.586	4.913	8.843
b:				5.437
c:	5.615	2.902	5.405	4.835
Space group	Hexagonal C_{3v}^4	Hexagonal C_{6h}^2	Hexagonal D_3^4	Orthorhombic C_{2v}^{12}
Formula unit Z	2	4	3	4
Bond distance (Å)				
Si—N (average)	1.738	1.730		1.714
Si—O (average)			1.610	1.623
Bond angle				
Si—N—Si	118.8	119.9		120
Si—O—Si			144	147.4
Effective charge Q^* in electron				
Si	1.48(0.85)	1.50(0.86)	1.40(0.81)	1.46(0.84)
N	6.89(1.12)	6.87(1.13)		6.90(1.10)
O			7.30(1.02)	7.25(1.01)

induced α to β transition were studied by Mirgorodsky, Baraton, and Quintard.[53] Similar analysis has also been carried out for Si_2N_2O.[54] Murakami and Sakka attempted molecular-orbital calculations on small clusters to determine interatomic potentials in silicon oxynitride glass.[55]

In this paper, we present results of calculations of the electronic structures of α-Si_3N_4, β-Si_3N_4, and Si_2N_2O crystals. Based on the electronic structure results, the optical properties of these crystals are also computed and compared with α-SiO_2. The optical and dielectric properties of ceramic materials have attracted much attention recently not only because of their relevance to materials application, but also because they provide further insight into the electronic structure and bonding in these crystals, and offer a viable means for materials characterization.[6,7,34,35,56–59] Most of the existing analyses of optical properties of ceramic films were based on simple dielectric models.[60–63] Our direct computation of the pure reference systems can certainly facilitate the improvement of these models. In Sec. II, we briefly outline the method of calculation. The results of electronic structure are presented and discussed in Sec. III; and that of the optical properties in Sec. IV. We make a few concluding remarks in Sec. V.

II. METHOD

We employ the self-consistent orthogonalized linear combination of atomic orbitals (OLCAO) method[64] to determine the electronic structure and use the resulting wave functions to obtain the optical spectra. Together with results from an earlier study on α-SiO_2 (and all other polymorphs of SiO_2) using the same method,[65] a detailed and insightful comparison among these four Si-based ceramic crystals can be made. The OLCAO method has been well described in the literature and should not be repeated.[64] Only a brief outline is given here. We may mention that similar calculations have been carried out for other fundamental ceramic crystals including Al_2O_3, MgO, $MgAl_2O_4$,[66,67] AlN,[68,69,75] ZrO_2,[70,76] Y_2O_3,[71] SiO_2,[65] TiO_2,[72] BN,[73] CaF_2,[74] SiC, BeO, GaN, and InN.[69] Very recently, we applied the same method to study the structural and optical properties of β-C_3N_4,[77] a crystal isostructural to β-Si_3N_4 that was theoretically predicted to have a hardness comparable to that of diamond.[78]

The OLCAO method is based on the density-functional theory with a local approximation.[79,80] The Wigner interpolation formula is used to account for the additional correlation effect.[81] The solid-state Bloch wave functions are expanded in terms of atom-centered atomic wave functions consisting of Gaussian-type orbitals. We use a full-basis set which comprises the minimal basis set plus additional orbitals corresponding to the next shell of quantum numbers.[64] The crystal potential and the charge density are also expressed as atom-centered functions consisting of s-type Gaussians whose expansion coefficients are determined numerically. The potential is iterated to self-consistency when the energy eigenvalues stabilize to less than 0.0001 eV. After self-consistency in the potential is achieved, the energy eigenvalues and wave functions are solved at a large number of k points in the Brillouin zone (BZ) for the calculation of the DOS and the optical conductivity function. It is well known that the local-density approximation (LDA) results in the underestimation of the band gap in the case of insulators and semiconductors.[82,83] In the present calculation for the optical properties, we do not attempt any correction procedure to adjust the band gap. Such a procedure probably will lead to some minor shift in the peak positions in the absorption spectra. Our major focus here is to make a comparative study of the four crystals. We nevertheless find our calculated absorption spectra uncorrected for the gap to be in rather close agreement with the measured data.

III. RESULTS ON ELECTRONIC STRUCTURES

The calculated self-consistent band structures of α-Si_3N_4, β-Si_3N_4, and Si_2N_2O crystals are shown in Fig. 2. Our band structure for β-Si_3N_4 is almost identical to the other self-consistent calculation by Liu and Cohen.[52] The top of the valence (VB) for β-Si_3N_4 is at a point along the Γ-A direction. For α-Si_3N_4, it is at the M point, and that of the Si_2N_2O is at the Γ point. The bottoms of the conduction band (CB) for all three crystals are at the Γ point. The general band structure of α- and β-Si_3N_4 are very similar, except that the former has twice as many

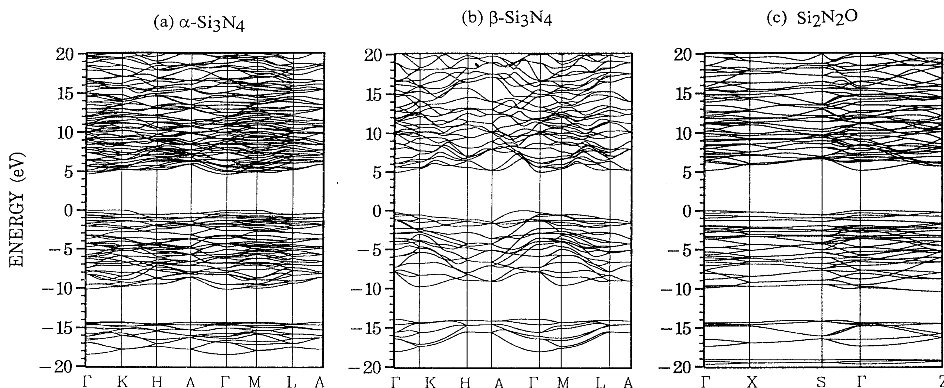

FIG. 2. Band structure of (a) α-Si_3N_4, (b) β-Si_3N_4, and (c) Si_2N_2O.

TABLE II. Comparison of calculated electronic structure of β-Si_3N_4, α-Si_3N_4, α-SiO_2, and Si_2N_2O crystals.

Crystal	α-Si_3N_4	β-Si_3N_4	α-SiO_2	Si_2N_2O
Top of VB	M	$\Gamma\rightarrow A$	K	Γ
Bottom of CB	Γ	Γ	Γ	Γ
E_g min. (eV)	4.63	4.96	5.59	5.20
E_g (direct at Γ)	4.67	5.25	5.91	5.20
Upper VB width (eV)	10.15	9.79	3.15,4.86	10.41
N 2s-band-width (eV)	4.16	4.12		3.31
O 2s-band-width (eV)			2.49	0.58
Effective-mass components:				
$m_e^*/m(\perp)$	0.93(Γ)	1.41 (Γ)	0.52 (Γ)	0.55(Γ)
$m_e^*/m(\parallel)$	0.81(Γ)	0.26 (Γ)	0.50 (Γ)	0.52 (Γ)
$m_h^*/m(\perp)$	large	large	-5.56 (K)	-1.52 (Γ)
$m_h^*/m(\parallel)$	-0.89 ($\Gamma\rightarrow A$) -0.55 ($M\rightarrow L$)	-1.41 ($\Gamma\rightarrow A$)	-1.31 (K)	-3.22 (Γ)

bands because the unit cell is twice as large. For Si_2N_2O, the O 2s band is located at slightly above -20 eV. As can be seen, the tops of the VB for all three crystals are very flat since they are derived from the more delocalized nonbonding 2p orbital of N. The effective-mass components for electrons (m_e^*) and holes (m_h^*) are estimated from band curvatures. For α-SiO_2 and Si_2N_2O crystals, the parallel ($\parallel$) and the perpendicular ($\perp$) components of the m_e^* are similar because the bottom of the single CB at Γ is derived mainly from the isotropic O 2s or N 2s orbitals. For the nitrides, m_e^* is much larger except for the $\parallel$ component in β-Si_3N_4, which has a rather small value of $0.25m_e$. The different stacking sequence in the crystal structures of α- and β-Si_3N_4 can partly explain the differences in effective-mass components. The hole effective mass m_h^* for all four crystals is large since the tops of the VB are comprised of localized N 2p or O 2P lone pairs. The comparison of different effective-mass components for m_h^* is complicated by the fact that only Si_2N_2O has the top of the VB at the Γ point of the BZ. The present band structures are more accurate than the earlier calculations.[45,46] The main VB width has increased, reflecting the effect of self-consistency in the po-

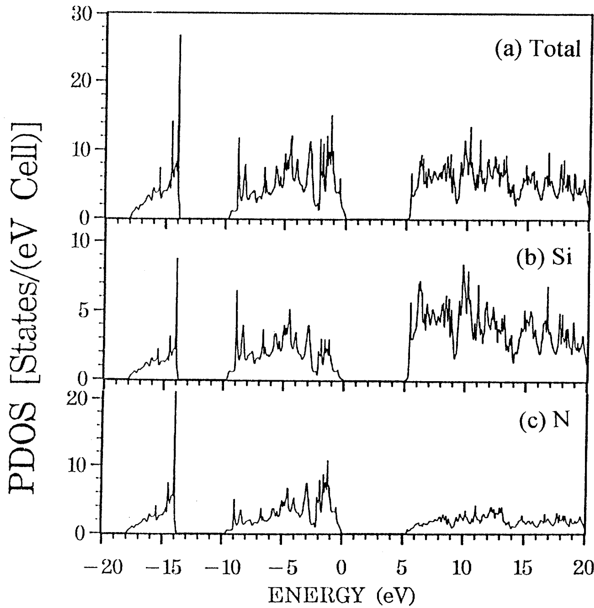

FIG. 3. DOS and partial DOS of β-Si_3N_4: (a) total, (b) Si, and (c) N.

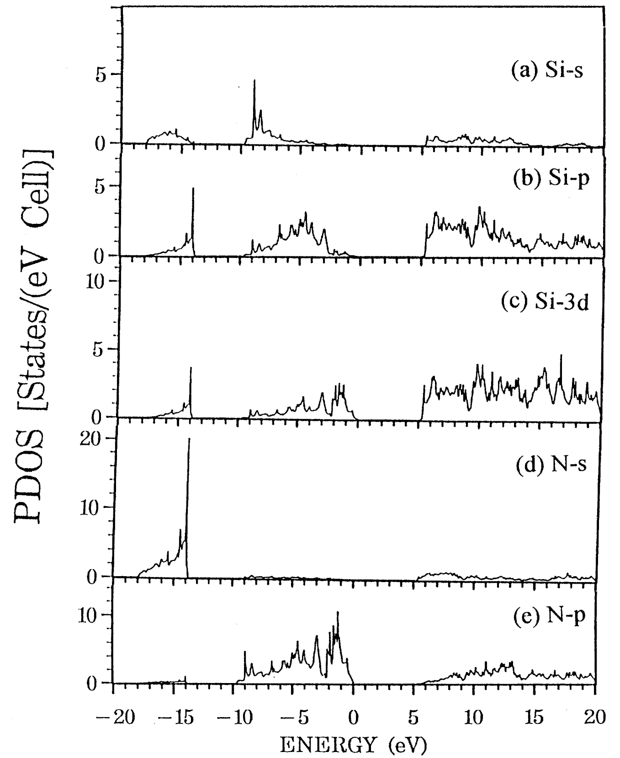

FIG. 4. Orbital-resolved partial DOS of β-Si_3N_4: (a) Si s, (b) Si p, (c) Si 3d, (d) N s, and (e) N p.

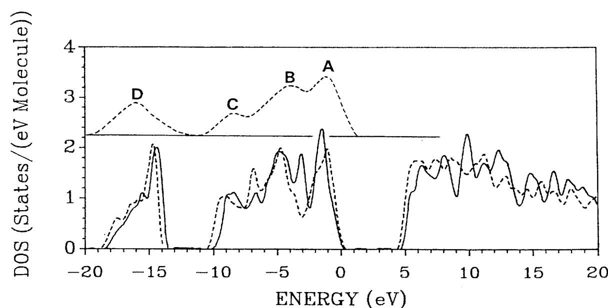

FIG. 5. Comparison of the DOS's of β-Si_3N_4 (solid line) and α-Si_3N_4 (dashed line). Upper dashed curve, XPS data for a-Si_3N_4 from Ref. 23.

tential. Information about the band gaps, bandwidths, effective-mass components, and effective charges (to be discussed below) for the four crystals including α-SiO_2 are summarized in Table II.

The calculated DOS's for β-Si_3N_4 and the atom-resolved partial DOS (PDOS) are shown in Figs. 3. To have a better idea about the nature of bonding, the orbital-resolved PDOS's are shown in Fig. 4. It should be pointed out that partitioning the DOS's into PDOS's is based on the Mulliken scheme,[84] which is only approximate. It is even less accurate when the basis function contains extended orbitals such as in the present case. The VB DOS consists of a deep N 2s band 4 eV wide centered at around -16 eV, and an upper VB of 10 eV wide consisting of Si 3p and N 2p bonding and nonbonding states. The CB DOS is dominated by Si 3d states mixed with the Si 3p and 4p states. Unlike the case of silicon oxide, the bonding and nonbonding bands in Si_3N_4 in the

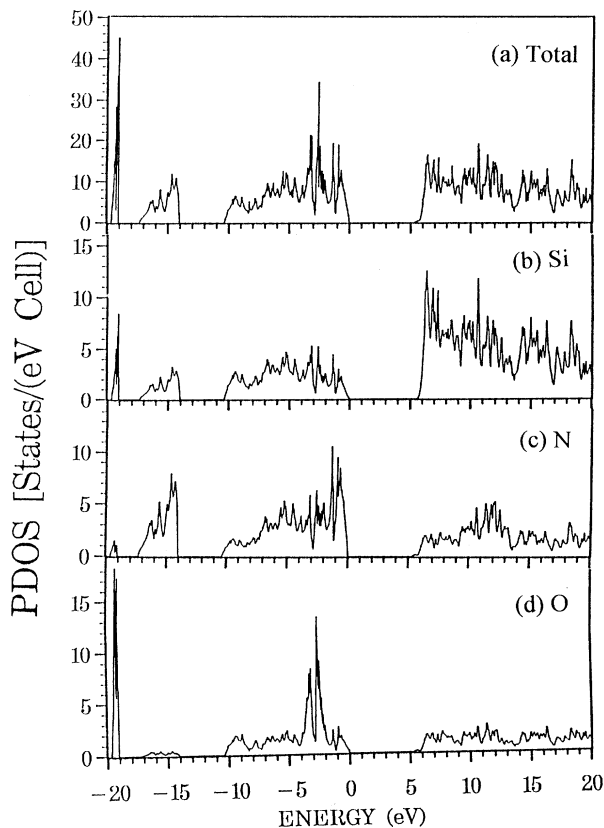

FIG. 6. DOS and partial DOS of Si_2N_2O: (a) total, (b) Si, (c), N, and (d) O.

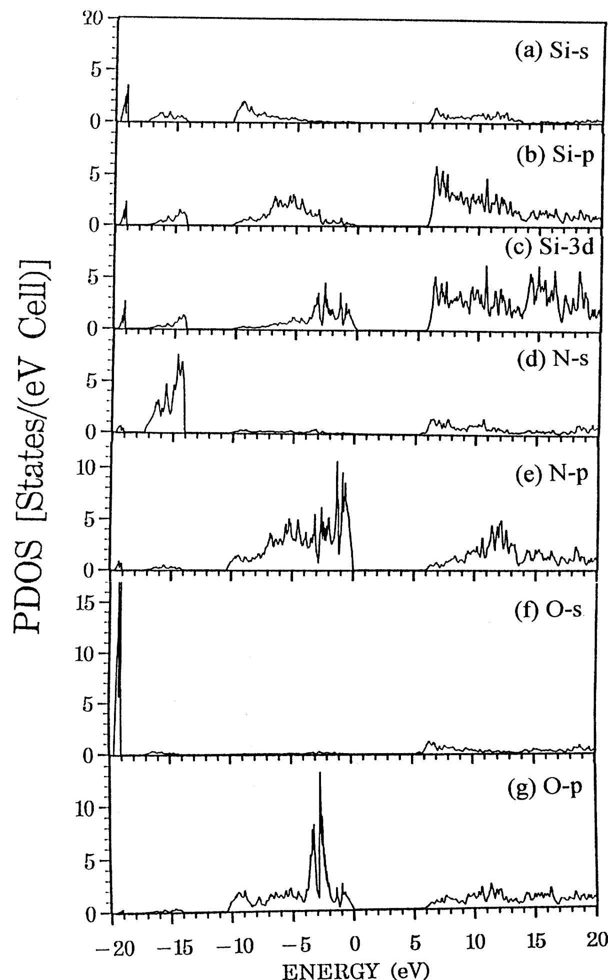

FIG. 7. Orbital-resolved partial DOS of Si_2N_2O: (a) Si s, (b) Si p, (c) Si 3d, (d) N s, (e) N p, (f) O s, and (g) O p.

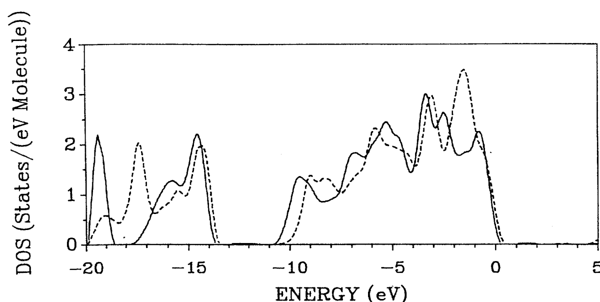

FIG. 8 Comparison of the DOS of Si_2N_2O (solid line) and the combination of β-Si_3N_4 and α-SiO_2 (Ref. 65) (dashed line).

upper VB are merged. The deep dip at -2.5 eV signifies the boundary of these two sets of bands. The nonbonding bands arise from the lone pair of N $2p$ orbitals. From the PDOS, it appears that Si $3d$ orbitals participate in the bonding at all energy ranges. This clearly shows that Si $3d$ orbitals are important in determining the overall electronic structure of Si_3N_4. However, as pointed out before,[45] this does not necessarily mean that the Si $3d$ orbital is crucial in the formation of the Si—N bond, but rather that it reflects a greater variational freedom in the basis expansion. The importance of the $pd\pi$ hybridization in Si—N and Si—O bonds has been a question of long standing and probably will not have a clear-cut answer. In a first-principles-type calculation such as in the present work, the orbital states are generally mixed, and it would be difficult to quantify the importance of the Si $3d$ orbital itself.

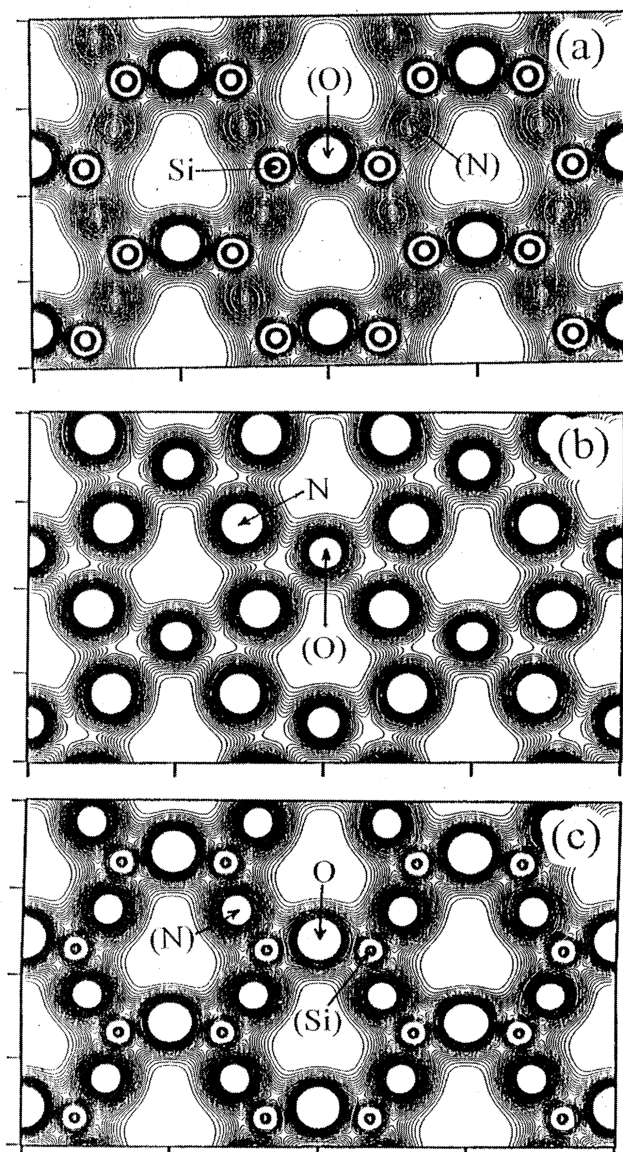

FIG. 9. Calculated valence charge density of Si_2N_2O in the [0001] planes containing (a) Si atoms, (b) N atoms, and (c) O atoms. Parentheses indicate the atom is an off-plane atom. The contour lines are from 0.01 to 0.25 by 0.005 in units of electrons.

The DOS and PDOS of α-Si_3N_4 are only slightly different from that of the β-Si_3N_4. This is illustrated in Fig. 5, where we compare the broadened total DOS of the α and β phases. The upper VB DOS of β-Si_3N_4 has five peaks at -1.4, -3.0, -4.9, -6.8, -8.9 eV. For the α phase, the width of the VB is increased by 0.4 eV and the five peaks shift slightly to -1.0, -3.8 (shoulder), -4.8, -6.9, and -9.3 eV. The N $2s$ bands for α-Si_3N_4 is also slightly shifted to the lower binding energy relative to β-Si_3N_4. Also shown in Fig. 5 are the x-ray-photoemission (XPS) spectrum of a-$SiN_{1.4}$ of Karchaer, Ley, and Johnson[28] at a photon energy of 87 eV. The low resolution for amorphous sample in XPS-type experiments prevents a detailed comparison on the structure. Still we can see the positions of the four peaks, marked A, B, C, and D agree well with the calculated DOS for crystalline samples. Increased experimental resolution may reveal the five-peak structure for the upper VB. The agreement is better with the α-Si_3N_4 than with β-Si_3N_4. It appears that α-Si_3N_4, with a wider distribution in bond lengths and bond angles, is closer in structure to a-SiN_x.

The VB structure of α and β and amorphous phases of Si_3N_4 were studied by Carson and Schnatterly[32] and Nithianandam and Schnatterly,[33] using soft-x-ray emission. The spectra they obtained for the three types of samples are very similar. Wiech and Simunek[44] measured the Si-K, Si-L, and N-K x-ray emission spectra of α- and β-Si_3N_4. Their main conclusion confirms that the upper VB has broad three-peak structures A, B, and C as shown in Fig. 5. The x-ray-emission spectroscopy (XES) data further indicate peak C to be Si $3s$ like, that peak B arises from Si $3p$ and N $2p$ and the peak A is composed of a mixture of Si $3s$, S $3d$, and N $2p$ components. This interpretation is consistent with the calculated orbital-resolved PDOS shown in Fig. 4.

The calculated total DOS, atom-resolved PDOS, and orbital-resolved PDOS of Si_2N_2O are shown in Figs. 6 and 7, respectively. The introduction of bridging O into the network greatly modifies the VB DOS profile. The upper VB is now wider than that of β-Si_3N_4 by about 0.6 eV, and there are more structures in the upper VB because of the presence of bonding and nonbonding O orbitals. In the early non-self-consistent calculation for Si_2N_2O,[46] the upper VB splits into two disjoint sections. This is no longer the case in the present calculation. However, the top of the VB remains distinct from the nonbonding N lone pair. To see how well the DOS of Si_2N_2O can be represented by the superposition of the DOS of Si_3N_4 and SiO_2, in Fig. 8 we plot the broadened DOS of Si_2N_2O and that of the weighted average of β-Si_3N_4 and α-SiO_2. It is clear that there are substantial differences in the peak positions and intensities in these two spectra. This is particularly true for the O $2s$ peak. In Si_2N_2O, the O $2s$ peak is much narrower and at a higher binding energy. This is because the bonding of N to Si in Si_2N_2O leads to a stronger Si potential as seen by

O. In the upper VB region, the superimposed curve shows a very strong peak at -1.4 eV due to the additive effect of the N $2p$ nonbonding peak in β-Si_3N_4 and the O $2p$ nonbonding peak in α-SiO_2. In Si_2N_2O, only the N $2p$ nonbonding peak remains at -0.9 eV; the O $2p$ nonbonding peak shifts to lower energy (higher binding energy) at -2.5 eV. On the other hand, the difference in the N $2s$ band is much smaller since the Si potential seen by a N atom in Si_2N_2O is only slightly different from that in β-Si_3N_4. In a series of Auger measurements of Si_3N_4 with varying O contents, Madden and Holloway[26] found that the O-related peak structure in the oxynitride is narrower and at a higher binding energy than the similar O peak in a-SiO_2, while there is little change in the N-related peak. Our calculated DOS for Si_2N_2O is fully consistent with their observation. Figure 8 clearly shows the importance of self-consistency in the potential in the electronic structure calculation for a multicomponent crystal, since a non-self-consistent calculation is unlikely to show such a difference.

The valence charge distributions for β-Si_3N_4 and α-SiO_2 have been presented before.[48,65] It was shown that both α-SiO_2 and β-Si_3N_4 have nonspherical charge-density distributions. Both ionic and covalent bonding characters are present. In Fig. 9, we present the valence charge density of Si_2N_2O crystal in the three planes perpendicular to the c axis, each containing Si, N, and O atoms, respectively. In each plane, the charge densities from the off-plane atoms show the bonding characteristic of the Si—N and Si—O bonds to be similar to those in Si_3N_4 and α-SiO_2. The covalently bonded network-type structure is very obvious. Of particular interest is the open channel of very low charge density running parallel to the c axis. Such an electron-density distribution generally indicates anisotropic transport properties.

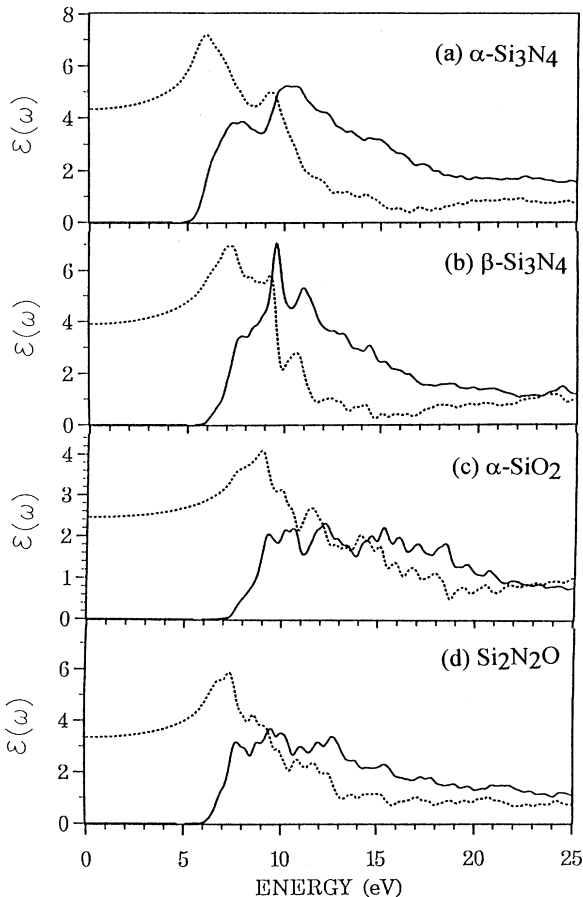

FIG. 10. Calculated real (dashed line) and imaginary (solid line) parts of the dielectric function: (a) α-Si_3N_4, (b) β-Si_3N_4, (c) α-SiO_2, and (d) Si_2N_2O.

In order to investigate the bonding in Si_3N_4, SiO_2, and Si_2N_2O crystals in more detail, we have estimated the effective charges on each atom by means of a direct space integration scheme using the self-consistent valence charge densities.[69,71] An ionic radius for each atom is first estimated from the charge map. The integrated charge within the sphere of that radius belongs to that ion. The rest of the charge in the crystal is apportioned to each ion in proportion to their spherical volume. This scheme, like any other scheme for effective charge, is approximate at best. Nevertheless, it provides a prescription to estimate the effective charge for each ion based on the self-consistent charge distribution. The results are listed in Table II. The Si—N bond is shown to be more covalent than the Si—O bond, because the Si in Si_3N_4 has a larger effective charge. The effective charges in Si_2N_2O are intermediate between Si_3N_4 and α-SiO_2, as expected. On the basis of these calculated effective charges, we may write the ionic formulas for the four crystals as α-$(Si^{+2.52})_3(N^{1.89})_4$, β-$(Si^{+2.50})_3(N^{-1.87})_4$, α-$(Si^{+2.60})(O^{-1.30})_2$, and $(Si^{+2.54})_2(N^{-1.90})_2(O^{-1.25})$. Thus the valence of O and N atoms in these compounds are not 2 and -3, respectively, as assumed in many empirical studies.

IV. RESULTS ON OPTICAL PROPERTIES

The optical properties of crystalline Si_3N_4 and Si_2N_2O are not well studied at all due to the lack of single-crystal samples for Si_3N_4 and Si_2N_2O. The most quoted measurement is still that of Phillip[85] on a-Si_3N_4 back in 1973, more than 20 years ago. More recently, better characterized thin films of silicon nitride and silicon oxynitride became available, but many of them contain H atoms. Limited optical measurements were carried out.[20,35,58,59,86] Because of the feasibility of using SiO_xN_y glass as a gradient index optical material,[20] intense research effort on the optical properties of Si_3N_4 and Si_2N_2O are expected. Since amorphous SiN_x or SiN_xO_y films are generally nonstoichiometric, and may even contain Si- or SiO_2-like regions, or void spaces, optical or dielectric measurements becomes a means of sample characterization provided the structure-properties relationship of the constitutional phases is well understood. Understanding the intrinsic optical properties of the pure reference crystals is certainly a matter of great importance. On the theoretical side, we are not aware of any serious calculation for the optical properties of these crystals. Empirical methods generally do not provide realistic wave functions

for detailed optical calculations.

Based on the *ab initio* wave functions, we have calculated the interband optical conductivities of these crystals, taking into account of the k dependence of the momentum matrix elements. All other optical functions such as real and imaginary parts of the dielectric functions, energy-loss functions, and the absorption coefficients can be obtained from the conductivity functions.[64] Our computational procedures are similar to those reported for α-SiO_2 (Ref. 65) and α-Al_2O_3 (Ref. 67). We have ignored the effect of the band-gap underestimation associated with the LDA theory in the present study. Our calculated optical results for α-Si_3N_4, β-Si_3N_4, α-SiO_2, and Si_2N_2O are shown in Fig. 10. Each section contains the real and imaginary parts of the dielectric function for photon energies up to 25 eV. The $\varepsilon_2(\omega)$ curve is evaluated first from the interband optical conductivity and the real part is obtained from the imaginary part by Kramers-Kronig conversion.[87] Within this frequency range, $\varepsilon_2(\omega)$ for β-Si_3N_4 has a sharp peak at 9.8 eV and less strong peaks at 7.8 and 11.0 eV. For the α phase, the main peak at 10.2 eV becomes much broadened, and the peak at 7.8 eV becomes stronger while the peak at 11.0 eV degenerates into a weak shoulder. For the Si_2N_2O crystal, there are many more structures in the $\varepsilon_2(\omega)$ curve, reflecting the multiple-peak structures in the VB DOS discussed in Sec. III. We can clearly identify structures as at 7.8, 9.6, 11.0, 12.0, 12.8, 13.9, and 15.5 eV. The peak structures in α-SiO_2 have been discussed before.[65] In α-SiO_2, the absorption spectrum is complicated by the presence of the excitonic peak.

The zero frequency limit of $\varepsilon_1(\omega)$ is the electronic part of the static dielectric constant $\varepsilon(0)$. The $\varepsilon(0)$ value averaged over the three Cartesian directions and their components in the directions parallel and perpendicular to the c axis are listed in Table III. We note that the $\varepsilon(0)$ of the nitrides are larger than that of oxides, as expected, and that $\varepsilon(0)$ of α-Si_3N_4 is larger than that of β-Si_3N_4. Of particular interest is the considerable optical anisotropy in nitrides. The parallel component is larger than the perpendicular component. This optical anisotropy must be related to the planar layered structure in both α-Si_3N_4 and β-Si_3N_4 discussed in Sec. I. Both α-SiO_2 and Si_2N_2O show no evidence of appreciable optical anisotropy.

The square root of $\varepsilon(0)$ is a good estimate of the refractive index in these crystals. For Si_3N_4 and Si_2N_2O systems, the only refractive index data available for comparison are for nonstoichiometric amorphous samples. These are listed in Table III. The general agreements are very consistent.

In Fig. 11, we compare the calculated optical conductivity of α-Si_3N_4 and β-Si_3N_4 with the optical data of Phillip[85] for a-Si_3N_4. The agreement is quite good for both the magnitude and shape of the spectrum up to 18 eV. Naturally, the structures in the calculated curve for crystals are absent in the data for amorphous samples. The $\varepsilon_2(\omega)$ curves for α-Si_3N_4 and β-Si_3N_4 are also in good agreement with a recent vacuum-ultraviolet (vuv) spectral measurement on polycrystalline samples of Si_3N_4 by French *et al.*[88]

For Si_2N_2O crystal, we cannot locate any measured data. Most existing optical measurements were on nonstoichiometric SiO_xN_y films.[7,20,58,59,89] It is highly desirable to have detailed optical measurements on crystalline samples of Si_2N_2O. A common practice is to assume the optical spectrum for Si_2N_2O can be represented by the superposition of the respective spectra of Si_3N_4 and α-SiO_2. In Fig. 12, we compare the calculated $\varepsilon_2(\omega)$ curve of Si_2N_2O with the average of α-Si_3N_4 and α-SiO_2 and the

TABLE III. Comparison of optical properties of β-Si_3N_4, α-Si_3N_4, α-SiO_2, and Si_2N_2O crystals.

Crystal	α-Si_3N_4	β-Si_3N_4	α-SiO_2	Si_2N_2O
$\varepsilon_1(0)$	4.33	3.90	2.45	3.34
$\varepsilon_1(0)(\parallel)$	4.45	4.01	2.45	3.33
$\varepsilon_1(0)(\perp)$	4.09	3.67	2.45	3.36
n, refractive index	2.08	1.97	1.57	1.83
n (experiment)		2.0[a], 1.99[b]	1.55	1.55-2.91[c]
		2.1[d], 2.04[e]	1.45 (glass)	1.68[f]
E_{op} (eV)	5.0–5.2	5.4–5.8	6.7–7.3	6.0
E_{op} (eV) (experiment)		4.4[g], 4.6[d]	8.8	5.2–5.7[h]
		4.0[a], 5.5[i]		5.25[j]

[a]Reference 90.
[b]Reference 56.
[c]Reference 57 for films of various thicknesses.
[d]Reference 58.
[e]Reference 35.
[f]Reference 7.
[g]Reference 40.
[h]Reference 57.
[i]Reference 89.
[j]Reference 6.

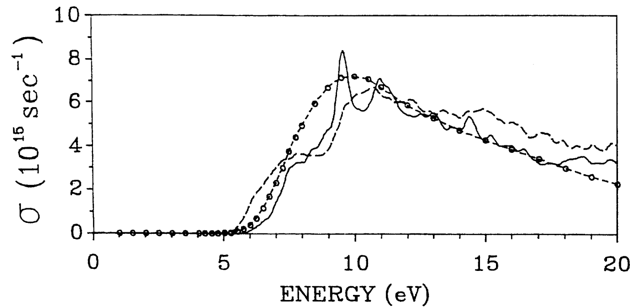

FIG. 11. Comparison of calculated $\sigma(\omega)$ for β-Si_3N_4 (solid line), α-Si_3N_4 (dashed line), and experimental data (circles) of Ref. 85 for a-Si_3N_4.

average of β-Si_3N_4 and a-SiO_2 without adjusting the band gap. As can be seen, the superimposed result is incapable of representing the absorption curve for Si_2N_2O crystal below 10 eV. It fails to reproduce the leading peak at 7.8 eV. It is precisely the absorption structures near the edge that control the refractive index of the material.

In Fig. 13, we plot the optical-absorption power which is proportional to $\varepsilon_2(\omega)\omega$ near the absorption edges for the four crystals. It is clear that there are tails in all four spectra before the onset of the sharp edge. The tail structures for α-SiO_2 and Si_2N_2O are larger than either of the nitrides. This is due to a single lower CB at Γ in oxides. The existence of the tail structure depends on the nature of the wave functions at the top of the VB and the bottom of the CB at the direct-gap minimum. It should be pointed out that in optical experiments, the gap is usually deduced from the extrapolation of the sharp absorption edge. The intrinsic tail structure indicates that the optical gap will be larger than the calculated intrinsic gap. This point is often ignored by may investigators when

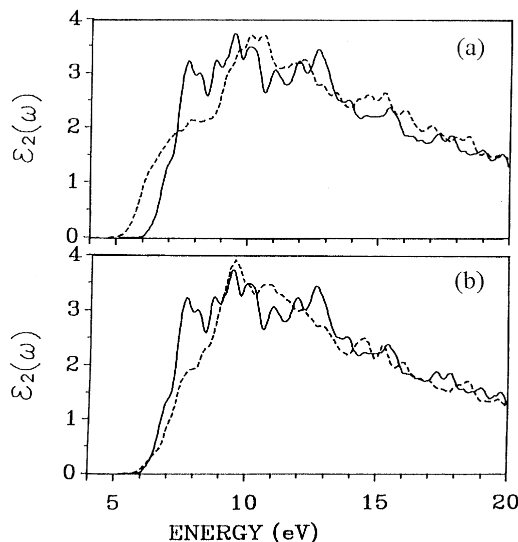

FIG. 12. Comparison of $\varepsilon_2(\omega)$ of Si_2N_2O with (a) average of α-Si_3N_4, and α-SiO_2; (b) average of β-Si_3N_4 and α-SiO_2.

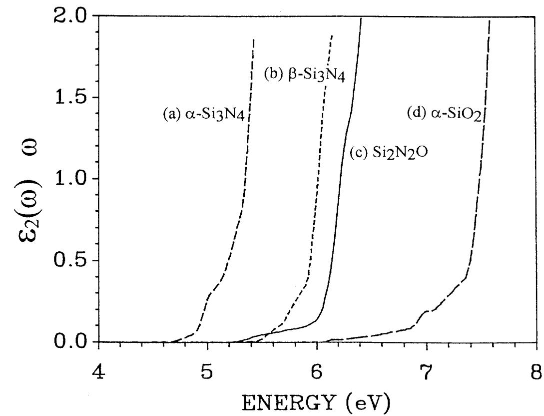

FIG. 13. The calculated absorption power near the threshold for the four crystals. (a) α-Si_3N_4, (b) β-Si_3N_4, (c) Si_2N_2O, and (d) α-SiO^2.

they compare the experimental gap with the calculated one. The problem is further confounded by the fact that the tail structure (the so called Ubach tail) in the experimental curve may also be due to the presence of defects, or due to finite temperature effect, i.e., phonon-assisted transitions. It is our contention that in oxides and other large-gap insulators, the calculated intrinsic gap is always smaller than the measured optical gap, even without considering the shortcoming of the LDA theory. In the present calculation, intrinsic band gaps of 4.63 and 4.96 eV (see Table II) for α-Si_3N_4 and β-Si_3N_4 are obtained, respectively. The extrapolated optical gaps according to Fig. 13 will be 5.0–5.2 eV for α-Si_3N_4 and 5.4–5.8 eV for β-Si_3N_4, respectively. This is in good agreement with the optical gap of 5.5 eV of Kurta, Hirose, and Osaka[89] and also Milek.[90] For α-SiO_2 and Si_2N_2O, the extrapolated optical gaps are 6.8–7.3 and 6.0 eV, respectively, compared to the direct gaps of 5.91 and 5.20 eV at Γ.

V. CONCLUSIONS

We have studied and compared the electronic structure of α-Si_3N_4, β-Si_3N_4, and Si_2N_2O crystals by means of first-principles self-consistent LDA calculations. The results show marked improvement over the older non-self-consistent calculations and are in good agreement with experimental measurements. We also show that the upper VB of nitrides may have five peak structures instead of only three. We show that Si—N and Si—O bonds in these crystals have both ionic and covalent characters with the Si—N bond more covalent, and hence a stronger bond. From the calculated effective charges, we deduce a more reasonable ionic formula for these crystals to be α-$(Si^{+2.52})_3(N^{-1.89})_4$, β-$(Si^{+2.50})_3(N^{-1.87})_4$, α-$(Si^{+2.60})(O^{-1.30})_2$, and $(Si^{+2.54})_2(N^{-1.90})_2(O^{-1.25})$.

We have also calculated the optical properties of these crystals and compared with the available experimental data. Our results will be useful as reference data for analyzing the optical properties of more complicated a-SiN_x and a-SiO_xN_y films. We emphasize the difference

between the calculated intrinsic gap and the experimental optical gap in insulating crystals. We show that the electronic structure and optical properties of the Si_2N_2O crystal cannot be adequately represented by a linear superposition of either α-Si_3N_4 or β-Si_3N_4 with α-SiO_2 because of the subtle interaction between Si, O, and N. It is further shown that both α-Si_3N_4 and β-Si_3N_4 possess substantial optical anisotropy which are absent in α-SiO_2 and Si_2N_2O.

The present result will be valuable for the study of a-SiN_x and for SiO_xN_y glasses, since the site-decomposed potentials from the self-consistent crystalline calculations are transferable and can readily be used to calculate the electronic structures of amorphous systems from first principles. By constructing appropriate structural models with different compositions, possibly containing real microstructures such as voids and different bonding configurations, and performing similar calculations on the electronic and optical properties, a much deeper understanding on the properties of these important ceramic materials can be achieved.

ACKNOWLEDGMENT

This work was supported by U. S. Department of Energy under Grant No. DE-FG02-84ER45170.

[1] *Progress in Nitrogen Ceramics,* Vol. 65 of *NATO Advanced Study Institute, Series E: Applied Sciences,* edited by F. L. Riley (Martinus Nijhoff, Boston, 1983).
[2] R. N. Katz, Science **208**, 84 (1980).
[3] *Ceramics for High Performance Applications II,* edited by J. J. Burke, E. M. Lenoe, and R. N. Katz (Brook Hill, Chestnut Hill, MA, 1978).
[4] *Silicon Nitride in Electronics,* edited by V. I. Belyi *et al.*, Materials Science Monographs Vol. 34 (Elsevier, New York, 1988).
[5] T. S. Eriksson and C. G. Granqvist, J. Appl. Phys. **60**, 2081 (1986).
[6] Q. A. Shams and W. D. Brown, J. Electrochem. Soc. **137**, 1244 (1990).
[7] M. del Giudice, F. Bruno, T. Cicinelli, and M. Valli, Appl. Opt. **29**, 3489 (1990)
[8] J. Weiss, Annu. Rev. Mater. Sci. **11**, 381 (1981).
[9] S. N. Ruddlesden and P. Popper, Acta Crystallogr. **11**, 465 (1958).
[10] O. Borgen, and H. M. Seip, Acta Chem. Scand. **15**, 1789 (1961).
[11] R. Marchand, Y. Laurent, and J. Lang, Acta Crystallogr. B **25**, 2157 (1969).
[12] I. Kohatsu and J. W. McCauley, Mater. Res. Bull. **9**, 917 (1974).
[13] S. Wild, P. Grieveson, and K. H. Jack, in *Special Ceramics 5,* edited by P. Popper (British Ceramic Association, Stoke-on-Trent, 1972), p. 385.
[14] R. Grun, Acta Crystallogr. B **35**, 800 (1979).
[15] I. Idrestedt and C. Brosset, Acta Chem. Scand. **18**, 1879 (1964).
[16] S. R. Srinivasa, L. Curtz, J. D. Jorgensen, T. G. Worlton, R. Beyerlein, and M. Billy, J. Appl. Crystallogr. **10**, 146 (1977).
[17] *Silicon Nitride Thin Insulating Films,* edited by V. J. Kapoor and K. T. Hankins (The Electrochemical Society, Pennington, NJ, 1987), Vol. 87.
[18] *LPCVD Silicon Nitride and Oxide Films, Materials and Applications,* edited by F. H. P. M. Habraken (Springer, Heidelberg, 1991).
[19] T. Okamoto, X. S. Ning, K. Sugamma, A. Koreeda, and Y. Miyamoto, in *Metal-Ceramic Interfaces,* edited by M. Rühle, A. G. Evans, M. F. Ashby and J. P. Hirth, Acta Scripta Metallurgica Proceeding Series Vol. 4 (Pergammon, New York, 1990), p. 182.
[20] T. Baak, Appl. Opt. **21**, 1070 (1982).
[21] L. Martin-Moreno, E. Martinez, J. A. Verges, and F. Yndurain, Phys. Rev. B **35**, 9683 (1987).
[22] J. P. Xantankis, S. Papadopoulos, and P. R. Mason, J. Phys. C **21**, L555 (1988).
[23] S. S. Makler, G. Martins da Rocha, and E. V. Anda, Phys. Rev. B **41**, 5857 (1990).
[24] J. Robertson, Philos. Mag. P **63**, 47 (1991).
[25] M. Misawa, T. Fukunaga, K. Niihara, T. Hirai, and K. Suzuki, J. Non-Cryst. Solids **34**, 313 (1979).
[26] H. H. Madden and P. H. Holloway, J. Vac. Sci. Technol. **16**, 618 (1979).
[27] N. Wada, S. A. Solin, J. Wong, and S. Prochazka, J. Non-Cryst. Solids **43**, 7 (1981).
[28] R. Karchaer, L. Ley, and R. L. Johnson, Phys. Rev. B **30**, 1896 (1984).
[29] S. Sakka, Ann. Rev. Mater. Sci. **16**, 29 (1986).
[30] B. Dunnett, D. I. Jones, and A. D. Stewart, Philos. Mag. B **53**, 159 (1986).
[31] G. M. Ingo, N. Zacchetti, D. della Sala, and C. Coluzza, J. Vac. Sci. Technol. A **7**, 3048 (1989).
[32] R. D. Carson and S. E. Schnatterly, Phys. Rev. B **33**, 2432 (1986).
[33] V. J. Nithianandam and S. E. Schnatterly, Phys. Rev. B **36**, 1159 (1987).
[34] P. Domashevskaya *et al.*, J. Non-Cryst. Solids **114**, 495 (1989).
[35] B. G. Bovard, J. Ramm, R. Hora, and F. Hanselmann, Appl. Opt. **28**, 4436 (1989).
[36] M. M. Guraya, H. Ascolani, G. Zampieri, J. I. Cisneros, J. H. Dias da Silva, and M. P. Cantao, Phys. Rev. B **42**, 5677 (1990).
[37] C. H. Seager and J. Kanicki, Phys. Rev. B **46**, 15 163 (1992).
[38] K.-C. Lin and S.-C. Lee, J. Appl. Phys. **72**, 5474 (1992).
[39] W. M. Arnoldbik, C. H. M. Maree, A. J. H. Maas, M. J. van den Boogaard, F. H. P. M. Habraken, and A. E. T. Kuiper, Phys. Rev. B **48**, 5444 (1993).
[40] C. Senemaud, M. Driss-khodja, A. Gheorghin, S. Harel, G. Dufour, and H. Roulet, J. Appl. Phys. **74**, 5042 (1993).
[41] M. D. Diatezua, P. A. Thiry, Ph. Lambin, and R. Caudano, Phys. Rev. B **48**, 8701 (1993).
[42] R. Saoudi, G. Hollinger, and A. Straboni, J. Phys. (France) III **4**, 881 (1994).
[43] M. M. Guraya, H. Ascolani, G. Zampieri, J. H. Dias da Silva, M. P. Cantao, and J. I. Cisneros, Phys. Rev. B **49**, 13 446 (1994).
[44] G. Wiech and A. Simunek, Phys. Rev. B **49**, 5398 (1994).
[45] S. Y. Ren and W. Y. Ching, Phys. Rev. B **23**, 5454 (1981).
[46] W. Y. Ching and S. Y. Ren, Phys. Rev. B **24**, 5788 (1981).

[47]Y. Xu, and W. Y. Ching, in *SiO_2 and Its Interfaces,* edited by S. T. Pantelides and G. Lucovsky, MRS Symposia Proceedings No. 105 (Materials Research Society, Pittsburgh, 1988), p. 181.
[48]Y. Xu and W. Y. Ching, Physica B **150**, 32 (1988).
[49]R. J. Sokel, J. Phys. Chem. Solids **41**, 899 (1980).
[50]J. Robertson, Philos. Mag. **44**, 215 (1981).
[51]I. Tanaka, K. Niihara, S. Nasu, and H. Adachi, J. Am. Ceram. Soc. **76**, 2833 (1993).
[52]A. Y. Liu and M. L. Cohen, Phys. Rev. B **41**, 10 727 (1990).
[53]A. P. Mirgorodsky, M. I. Baraton, and P. Quintard, Phys. Rev. B **48**, 13 326 (1993).
[54]A. P. Mirgorodsky, M. I. Baraton, and P. Quintard, J. Phys. Condens. Matter **1**, 10 053 (1989).
[55]M. Murakami and S. Sakka, J. Non-Cryst. Solids **101**, 271 (1988).
[56]R. W. Knoll and C. H. Henager, Jr., J. Mater. Res. **7**, 1247 (1992).
[57]V. A. Gritsenko, N. D. Dikovskaja, and K. P. Magilnikoo, Thin Solid Films **51**, 353 (1978).
[58]A. L. Shabalov, M. S. Feldman, and M. Z. Bashirov, Phys. Status Solidi B **145**, K71 (1988).
[59]Yi-Ming Xion *et al.*, Thin Solid Films **206**, 248 (1991).
[60]D. E. Aspnes and J. B. Theeten, J. Appl. Phys. **50**, 4928 (1979).
[61]Z. Yin and F. W. Smith, Phys. Rev. B **42**, 3658 (1990); **42**, 3666 (1990).
[62]U. Teschner, Phys. Status Solidi A **121**, 641 (1990).
[63]A. Sassela, Phys. Rev. B **48**, 14 208 (1993).
[64]W. Y. Ching, J. Am. Ceram. Soc. **73**, 3135 (1990).
[65]Y.-N. Xu and W. Y. Ching, Phys. Rev. B **44**, 11 048 (1991).
[66]Y.-N. Xu and W. Y. Ching, Phys. Rev. B **43**, 4461 (1991).
[67]W. Y. Ching and Y.-N. Xu, J. Am. Ceram. Soc. **77**, 404 (1994).
[68]W. Y. Ching and B. N. Harmon, Phys. Rev. B **34**, 2080 (1986).
[69]Y.-N. Xu and W. Y. Ching, Phys. Rev. B **48**, 4335 (1993).
[70]F. Zandiehnadem, R. A. Murray, and W. Y. Ching, Physica B **150**, 19 (1988).
[71]Y.-N. Xu and W. Y. Ching, Phys. Rev. Lett. **65**, 895 (1990).
[72]S.-D. Mo and W. Y. Ching, Phys. Rev. B **51**, 13 023 (1995).
[73]Y.-N. Xu and W. Y. Ching, Phys. Rev. B **44**, 7787 (1991).
[74]F. Gan. M.-Z. Huang, Y.-N. Xu, W. Y. Ching, and J. G. Harrison, Phys. Rev. B **45**, 8248 (1992).
[75]S. Loughin, R. H. French, W. Y. Ching, Y.-N. Nu, and G. A. Slack, Appl. Phys. Lett. **63**, 1182 (1993).
[76]R. H. French, S. J. Glass, F. S. Oguchi, Y.-N. Xu, and W. Y. Ching, Phys. Rev. B **49**, 5133 (1994).
[77]H. Yao and W. Y. Ching, Phys. Rev. B **50**, 11 231 (1994).
[78]M. L. Cohen, Phys. Rev. B **32**, 7988 (1985); A. Y. Liu and M. L. Cohen, Science **245**, 841 (1989).
[79]P. Hohenberg and W. Kohn, Phys. Rev. **13**, B864 (1964).
[80]W. Kohn and L. J. Sham, Phys. Rev. **140**, A1133 (1965).
[81]E. Wigner, Phys. Rev. **46**, 1002 (1934).
[82]M. S. Hybersen and S. G. Louie, Phys. Rev. Lett. **55**, 1418 (1985); Phys. Rev. B **34**, 5390 (1986); **37**, 2733 (1988).
[83]R. W. Godby, M. Schluster, and L. J. Sham, Phys. Rev. Lett. **56**, 2415 (1986); Phys. Rev. B **36**, 6497 (1987); **37**, 10 159 (1988).
[84]R. S. Mulliken, J. Am. Chem. Soc. **77**, 887 (1954).
[85]J. Petalas and S. Logothetidis, Phys. Rev. B **50**, 11 801 (1994).
[86]H. R. Phillip, J. Electrochem. Soc. **120**, 295 (1973).
[87]Our calculated results for $\varepsilon_1(\omega)$ for α-SiO_2 are slightly different from those presented in Ref. 65 because of the improvement in the K-K conversion. The previous calculation contains a small error which affects the $\varepsilon_1(\omega)$ value in the conversion process.
[88]R. H. French, R. M. Canon, L. K. Denoyer, and Y.-M. Chiang, Solid State Ionics **75**, 13 (1995).
[89]H. Kurta, M. Hirose, and Y. Osaka, Jpn. J. Appl. Phys. **20**, L811 (1981).
[90]J. T. Milek, *Handbook of Electronic Materials* (IFI/Plenum, New York, 1971), Vol. 3.